Pharmacogn. Mag.
A multifaceted peer reviewed journal in the field of Pharmacognosy and Natural Products
www.phcog.com | www.phcog.net

ORIGINAL ARTICLE

A Rapid and Efficient Approach Based on Ultra-High Liquid Chromatography Coupled with Mass Spectrometry for Identification *in vitro* and *in vivo* Constituents from *Shizao* Decoction

Yu-Mei Wang, Qi Liu, Wen-Hao Fu, Ai-Hua Zhang[1]

Qiqihar Academy of Medical Sciences, The Research Institute of Medicine and Pharmacy, Qiqihar Medical University, Qiqihar, Heilongjiang, [1]National Chinmedomics Research Center, Sino-America Chinmedomics Technology Collaboration Center, National Traditional Chinese Medicine Key Laboratory of Serum Pharmacochemistry, Metabolomics Laboratory, Heilongjiang University of Chinese Medicine, Harbin, China

Submitted: 07-08-2019 Revised: 04-09-2019 Published: 11-02-2020

ABSTRACT

Introduction: *Shizao* decoction (SZD) is a classic Chinese prescription which used in multiple kinds of ascites and edema caused by liver cirrhosis, chronic nephritis, etc. However, considering edema and new application of cancer ascites SZD is worth further investigating. **Materials and Methods:** In this paper, a powerful ultra-high liquid chromatography coupled with electrospray ionization quadrupole time-of-flight mass spectrometry based on the PeakView tool combined with multivariate data processing approach was employed to clarify the chemical constituents and the ingredients absorbed into blood after oral administration of SZD. **Results:** As a result, a total of 91 compounds (35 ions in positive mode and 56 ions in negative mode) of SZD *in vitro* were successfully identified. Besides, 25 constituents absorbed into blood were tentatively characterized. Among the characterized ingredients, flavonoids, prenol lipids, coumarins, and derivatives and benzopyrans were also detected, respectively. Of note, some constituents absorbed into blood played a critical role in cancer therapy. **Conclusion:** Established method was suitable for the rapid analysis and characterization of SZD constituents, and it provided meaningful chemical information for further pharmacology study of SZD.

Key words: Constituents, decoction, mass spectrometry, traditional Chinese medicine, ultra-high liquid chromatography

SUMMARY

- The established ultra-high liquid chromatography coupled with electrospray ionization quadrupole time-of-flight mass spectrometry analysis combined with multivariate data processing approach was suitable for the rapid identification of constituents from SZT *in vitro* and *in vivo*.

Abbreviation used: SZD: Shizao decoction; TCM: Traditional Chinese medicine; UHPLC-ESI-Q-TOF-MS: ultra-high liquid chromatography coupled with electrospray ionization quadrupole time-of-flight mass spectrometry; IDA: information-dependent acquisition; IST: ion source temperature; ISVF: ion spray voltage floating; DP: declustering potential; CE: collision energy; GS 1: nebulizer gas; GS 2: auxiliary gas; CUR: curtain gas; BPCs: base peak chromatograms

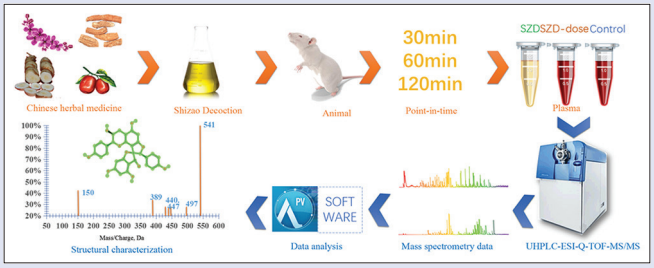

Correspondence:

Dr. Qi Liu,
Qiqihar Academy of Medical Sciences, The Research Institute of Medicine and Pharmacy, Qiqihar Medical University, Bukui Street 333,
Qiqihar, Heilongjiang, China.
E-mail: liuqi_hlj@163.com
Prof. Ai-Hua Zhang,
National Chinmedomics Research Center, Sino-America Chinmedomics Technology Collaboration Center, National Traditional Chinese Medicine Key Laboratory of Serum Pharmacochemistry, Metabolomics Laboratory, Heilongjiang University of Chinese Medicine, Heping Road 24, Harbin, China.
E-mail: aihuatcm@163.com
DOI: 10.4103/pm.pm_329_19

Access this article online
Website: www.phcog.com
Quick Response Code:

INTRODUCTION

Traditional Chinese medicine (TCM) has made a great contribution to the prevention and treatment of diseases for thousands of years. What makes TCM unique was that it expressed its synergistic effects through multiple components and multiple targets. Therefore, the screening of essential constituents and bioactive components was the first line to further study of TCM. Recently, with the emergence of rapid analytical techniques such as liquid chromatography-mass spectrometry/mass spectrometry (LC-MS/MS) and gas chromatography (GC)-MS/MS, and a forceful experimental method named serum pharmacochemistry, the bioactive ingredients of TCM became possible to clarify. Hence, up to now, the bioactive components in rat serum after oral administration of multifarious TCM prescriptions such as Xiaochaihu Tang,[1] FangjiHuangqi Tang,[2] Yin-Chen-Hao-Tang,[3] Simiao Wan,[4] Zhizhu Wan,[5] Kaixin San,[6,7] and Shengmai San[8-10] and single herbs such as leaves of *Radix*

Cite this article as: Wang YM, Liu Q, Fu WH, Zhang AH. A rapid and efficient approach based on ultra-high liquid chromatography coupled with mass spectrometry for identification *in vitro* and *in vivo* constituents from *Shizao* decoction. Phcog Mag 2020;16:148-55.

Astragali,[11] *Phellodendri amurensis* cortex,[12] *Panax notoginseng*,[13] *Acanthopanax Senticosus stem*,[14] *Radix Polygalae*,[15] and corn silk[16-18] have been screened successfully.

Shizao decoction (SZD), a traditional Chinese herb formula from "Shanghan Lun," one of the four medical collections from ancient China, was composed of four kinds of active Chinese herbs, including *Daphne genkwa* Sieb. et Zucc. (Yuanhua), *Euphorbia kansui* T. N. Liou ex T. P. Wang (Gansui), *Euphorbia pekinensis* Rupr. (Jingdaji), and *Fructus Ziziphus jujuba* Mill. (Dazao). It was widely used in the treatment of exudative meningitis, tuber culouspleuritis, various kinds of hydrothorax, ascites, and even hyposarca caused by liver cirrhosis, chronic nephritis, and advanced schistosomiasis in past years. However, because of the remarkable toxicity of Gansui,[19] Yuanhua[20] and Jingdaji,[21] SZD was used with extraordinary caution in the clinical study. Recently, SZD has been attracted much more attention in clinical and scientific research fields.

As is well-known that, chemical constituents are the material basis of TCM; however, up to now, the constituents of SZD *in vitro* and *in vivo* are not very clear yet. Therefore, the comprehensive research of the constituents *in vitro* and *in vivo* is helpful for the pharmacological and mechanism studies of SZD. In this case, we wonder whether several fulfilling compounds of SZD would be detected in rat serum or not. Hence, a rapid and sensitive ultra-high LC coupled with electrospray ionization quadrupole time-of-flight MS (UHPLC-ESI-Q-TOF-MS) technology combined with an automated multivariate analysis approach based on the serum pharmacochemistry method was employed to rapidly screen and analyze the multiple absorbed bioactive components of SZD after oral administration. These results filled the gaps in the chemical study and provided helpful data for further pharmacological and action mechanism research of SZD.

EXPERIMENTAL

Chemicals, reagents, and materials

Acetonitrile (HPLC grade) and methanol (HPLC grade) were purchased from Merck Company (Darmstadt, Germany). Formic acid (FA) (HPLC grade) was purchased from Fisher Scientific Company (USA). The distilled water (18.2 MΩ) was purified by a Milli-Q system (Millipore, Bedford, MA, USA). Oasis HLB SPE C_{18} was purchased from Waters Corporation (Milford, USA). Yuanhua, Gansui, Jingdaji, and Dazao were purchased from Harbin Sankeshu Drugstore (Heilongjiang, China) and identified by Doctor Qi Liu, Qiqihar Medical University.

Sample preparation

The dried powder of Gansui, Yuanhua, and Jingdaji was mixed according to a ratio of 1:1:1, and then, 10 times of 50% ethanol were added to the mixture powder and extracted by ultrasonic for twice, each time lasted for 1 h. Then, 1000 g of Dazao was added to 10 times of distilled water and extracted by a reflux extractor for 2 h. Finally, the above two kinds of solutions were mixed and concentrated to 1.0 g/mL by a rotary evaporation at 35°C. At the same time, 10 g of Yuanhua, Gansui, and Jingdaji were extracted through ultrasonic by 10 times of 50% ethanol for twice each time lasted for 1 h. Besides, 10 g of Dazao powder were extracted for 2 h by a reflux by 10 times of distilled water. Then, SZD sample and the individual drug samples were obtained, respectively. Finally, after diluted and filtered through a 0.22 μm membrane, the SZD sample and the individual drug samples were finally injected into the UHPLC-ESI-Q-TOF-MS system.

Animal handling

Twenty-four male Wistar rats (weighing 200 ± 20 g, 20 w) were purchased from the experimental animal center of Qiqihar Medical University. The animals were housed under controlled environmental conditions (temperature of 24°C ± 2°C humidity of 60% ± 5%; 12 h/12 h dark/light cycle) to acclimatize for 1 week. All the rats were fed with standard diet and water *ad libitum*. After acclimatization, all the animals were divided into four groups of six rats each as follows: dosed Group 1, dosed Group 2, dosed Group 3, and control group. The rats of dosed groups were administrated with SZD extract (1.0 mL/100 g) orally for 7 days. At the same time, the rats of the control group were administrated with CMC-Na solution alone under the same conditions. After the administration of 30 min, 60 min, and 90 min, rats of dosed Group 1, dosed Group 2, and dosed Group 3 were deeply anesthetized by 3% pentobarbital sodium and then sacrificed, respectively. Blood was collected from the abdominal aorta and placed for 1 h after centrifuged at 4000 rpm for 20 min at 4°C; the supernatant serum was then separated. Finally, the obtained serum was stored at −80°C until analysis. All animal care and experimental procedures were carried out in compliance with the Institutional Animal Care and Use Committee of Qiqihar Medical University.

Preparation of serum sample for ultra-high liquid chromatography coupled with electrospray ionization quadrupole time-of-flight mass spectrometry/mass spectrometry analysis

After thawed, all the serum samples were centrifuged at 13,000 rpm for 10 min at 4°C. Then, 40 μL of phosphoric acid was added to 1 mL of serum sample and vortex-mixed for 60 s. After that, the mixed solution was extracted by an Oasis HLB solid-phase extraction C_{18}-column (Waters, USA), which was preactivated by 2 mL of methanol and 2 mL of distilled water. Then, 1 mL of 100% distilled water was used to wipe off the impurity, and 2 mL of 100% methanol was used to eluting the aimed ingredients. Afterward, the collected eluent was dried under a stream of nitrogen gas at 45°C, and each dried sample was further redissolved in 200 μL of 80% methanol. Finally, the solution was centrifuged at 13,000 rpm for 10 min at 4°C and then filtered through a 0.22 μm membrane, 3uL of serum sample was injected into the UHPLC-ESI-Q-TOF-MS/MS system. Besides, all the serum samples were equally mixed to gain a QC sample, which was injected each five injections during the detection.

Ultra-high liquid chromatography coupled with electrospray ionization quadrupole time-of-flight mass spectrometry/mass spectrometry conditions

The analysis was performed on an ultra-performance LC-30A system (Shimadzu Company, Japan) coupled with an accurate tripleTOF 4600 mass system (AB SCIEX, USA) equipped with an electrospray ion source interface. The chromatographic separation was conducted on an ACQUITY UPLC HSS T_3 column (2.1 mm × 100 mm, 1.8 um, Waters Corporation, Milford, USA) at 40°C with a velocity of 0.4 mL/min. The mobile phase was composed of solvent A (0.1% FA in acetonitrile) and solvent B (0.1% FA in water) under gradient elution conditions: 0.01–3.00 min, 1%–10% A; 3.00–9.00 min, 10%–30% A; and 9.00–18.00 min, 30%–100% A. The injection volume was set at 3 μL.

After chromatographic separation, the column eluent of each sample was further analyzed in positive ion mode and negative ion mode. During the experiment, a comprehensive acquisition method named information-dependent acquisition (IDA) was employed to gain TOFMS

and MS/MS data in one injection. The parameters of TOFMS under a positive ion mode were as follows: ion source temperature (IST) was maintained at 600°C, ion spray voltage floating (ISVF) was set at 5.5 KV, declustering potential (DP) and collision energy (CE) were maintained at 100V and 10V, respectively. Pressures of nebulizer gas (GS 1), auxiliary gas (GS 2), and the curtain gas (CUR) were maintained at 55 psi, 55 psi, and 30 psi, respectively. The TOFMS accumulation time was 150 ms, and the complete scan was performed within m/z 100–1000 Da. Besides, the parameters of IDA-MS/MS were as below: DP, CE, and CES were 100V, 40V, and 20V, respectively. The MS/MS accumulation time was run within 80 ms. The parameters under negative ion mode were as follows: IST was maintained at 600°C, ISVF was set at −4.0KV, DP, and CE were set at 100V and 10V, pressures of GS 1, GS 2, and CUR were set at 65 psi, 65 psi, and 30 psi, respectively. CE and CES were maintained at −40V and 20V. During the IDA-MS/MS analysis, a dynamic background subtracting method which could differentiate the background and matrix-related MS/MS ions from endogenous or exogenous components intelligently was employed. Moreover, the top ten strongest fragment ions of more than 100 cps during 50–1000 amu in every accumulation time were given priority to matching with the IDA criteria. In addition, calibration was operated through a Calibrant Delivery System each five samples. All the acquisitions were conducted by Analyst TF 1.7.1 software (AB Sciex Corporation, CA, USA).

Data analysis

All obtained data files were processed using Progenesis QI 2.0 (Waters Corporation, Milford, MA, USA). After the data loading forms (POS: +H, +NH4, +Na, +K, 2M+H; NEG:-H, +Cl, +FA-H) were selected, the data were further processed by peak matching, peak alignment, and peak extraction, and then, a matrix containing retention time, mass number, and peak intensity information were obtained. Then, a list including compound's name, molecular formula and m/z of constituents from SZD were imported into Progenesis SDF Studio and a new SDF database was established successfully.. Next, after matching by MS, MS/MS information and confirmed by Progenesis QI, the chemical constituents of SZD were finally identified. As the same way, constituents of Yuanhua, Gansui, Jingdaji, and Dazao samples were identified, respectively. After comparing the identified results with each other, the constituents source was located. Next, data files of three dosed groups and a control group were imported into Progenesis QI 2.0 software, after peak matching, peak alignment and peak extraction, ions which present in dosed groups but absent in control group were regarded as the potential. Finally, the detail information of constituents migrating into blood were found out and finally identified by matching with MS, MS/MS, and network databases.

RESULTS AND DISCUSSION

Based on the satisfying acquisition conditions, the approving chromatography and mass spectrum results were orderly obtained. The base peak chromatograms (BPCs) of SZD, Yuanhua, Gansui, Jingdaji, and Dazao were shown in Figure 1. As the results displayed, 91 peaks in SZD containing flavonoids, fattyacyls, coumarins and derivatives, organic compounds, organooxygen compounds, carboxylic acids and derivatives, imidazopyrimidines, etc., were successfully identified in sequence using the UHPLC-ESI-Q-TOF-MS/MS technique. The multiple classes of constituents revealed the complexity of TCM prescription. Among the identified constituents of SZD, 40 of them were flavonoids, accounting for 44% of the identified constituents. In the second place, 9 of them were fatty acyls, accounting for 10%. This revealed that flavonoids and fatty acyls may play an important role in SZD. Moreover, among the identified constituents, 85 constituents were from Yuanhua, accounting for 93% of the detected compounds, indicating that Yuanhua may play a critical role in the constituents

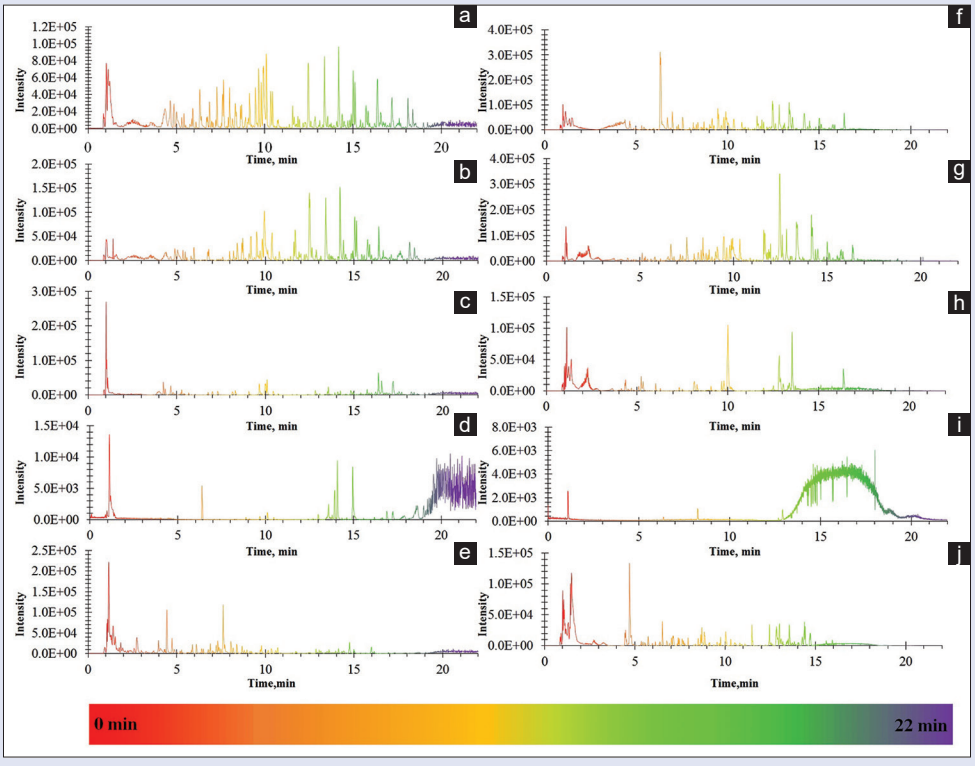

Figure 1: The base peak chromatograms of *Shizao* decoction (a: POS and f: NEG), Yuanhua (b: POS and g: NEG), Gansui (c: POS and h: NEG), Jingdaji (d: POS and i: NEG), and Dazao (e: POS and j: NEG) under. POS: Positive ion mode, NEG: Negative ion mode

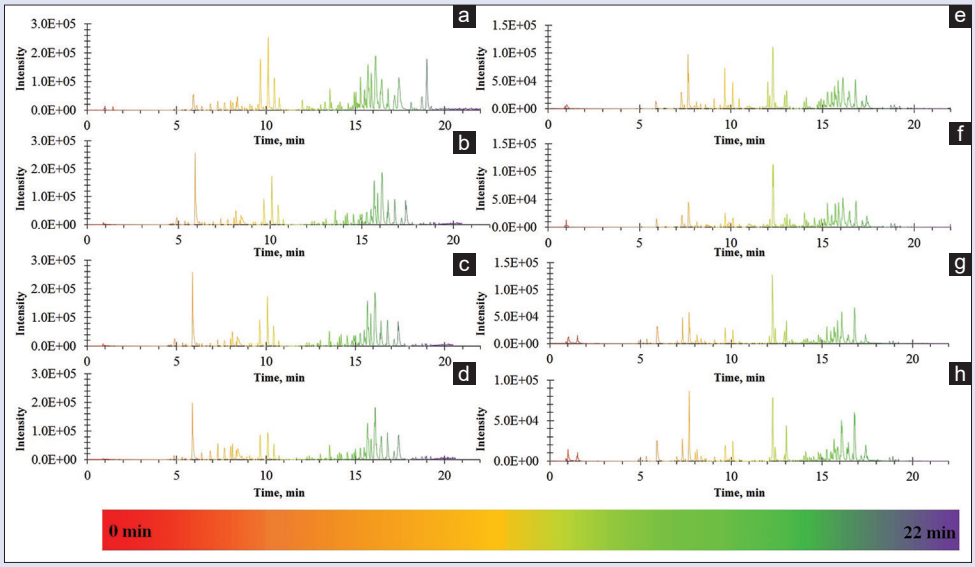

Figure 2: The base peak chromatograms of control serum sample (a: POS and e: NEG), dosed serum of 30 min (b: POS and f: NEG), 60 min (c: POS and g: NEG) and 90 min (d: POS and h: NEG) under. POS: Positive ion mode, NEG: Negative ion mode

of SZD. Twenty-six constituents were from Gansui, 20 constituents were from Dazao, and 18 constituents were from Jingdaji. Besides, 12 constituents including L-Proline, 7,8-dihydroxy-4-methylcoumarin, adenine, norharmane, 9-oxo-10E,12Z,15Z-octadecatrienoic acid, heptadecanoic acid, 9,12-Octadecadiynoic acid, monolinolenin (9c, 12c, 15c), 13-keto-9Z,11E-octadecadienoic acid, oleamide, erucamide, and asperulosidic acid were the common constituents from Yuanhua, Gansui, Jingdaji, and Dazao. The detail information of the identified results of SZD was shown in Table S1.

The control serum sample, dosed serum of 30 min, 60 min, and 90 min were orderly analyzed, and the BPCs under positive ion mode and negative ion mode were shown in Figure 2. At first sight, there were no significant differences among the peaks of control serum sample and dosed serum samples in Figure 2 at first sight, because that BPC was a simplified visual map of total ion chromatogram which owns continuous point of the strongest ions in the mass spectrum at each time point, and it was mainly employed to better understanding the contour differences among different samples. Besides, the content of constituent migrating into blood was very little and owns extremely low intensity. Hence, we could not found obvious differences in BPCs in Figure 2. The data of control serum, dosed serum of 30 min, 60 min, and 90 min were processed by Progenesis QI 2.0 software and PeakView software. The results of dosed serum of 30 min, 60 min, and 90 min were severally compared with control serum. Take the identification process of peak 4 detected *in vitro* and *in vivo,* for example, under positive ion mode, the retention time was 4.07 min, and the m/z was 193.0504. The ion's molecular formula was confirmed as $C_{10}H_8O_4$ through speculated through formula finder based on the elemental composition and fractional isotope abundance. Next, the unsaturation degree was calculated as 7, suggesting that it may be a ring compound. Moreover, the main MS/MS fragments were m/z 175, m/z 147, m/z 131, m/z 119, m/z 91, m/z 77, and m/z 131, indicating that the surplus fragments may be $-C_{10}H_7O_3+$, $-C_9H_7O_2+$, $-C_9H_7O+$, $-C_9H_{11}+$, $-C_6H_3O+$, $-C_6H_5+$, and $-C_4HO+$, respectively. At last, after matching with online and native databases, the structure was finally confirmed, and it was identified as 7,8-dihydroxy-4-methylcoumarin. The detail MS/MS fragments of 7,8-dihydroxy-4-methylcoumarin and other typical constituents were displayed in Figure 3.

Based on the identification results, 25 constituents including 7,8-dihydroxy-4-methylcoumarin, phomoeuphorbin C, helioscopinolide A, neochlorogenic acid, asperulosidic acid, 7,8-dihydroxycoumarin, phomoeuphorbin A, ent-Robinetinidol, 2-hydroxycinnamic acid, luteolin-4'-O-glucoside, hyperoside, scutellarin, oroxin A, quercetin 3-O-beta-D-glucose-6'-acetate, apiin, pratensein-7-O-glucoside, baicalin, genkwanol A, luteolin 7,3'-dimethyl ether 5-glucoside, cosmosiin, kaempferol 7-O-alpha-L-rhamnopyranoside, tiliroside, 3-epilitsenolide D2, dihydroxy-2-(4-hydroxyphenyl) chromen, and hispidulin were figured out to be the constituents absorbed into blood. Among the constituents migrating into blood, 51.7% of them were flavones, 10% were coumarins and derivatives, 10% were prenol lipids, and 9% were benzopyrans, besides, there were still other kinds of constituents such as lactones, organooxygen compounds, cinnamic acids and derivatives, isoflavonoids and 2-arylbenzofuran flavonoids compounds. However, the constituents unmigrating into blood of SZD mainly containing fatty acyls, carboxylic acids and derivatives, imidazopyrimidines, indoles and derivatives, etc. The results indicate that flavones, coumarins, and derivatives, prenol lipids, and benzopyrans of SZD were much more easily migrating into blood in comparison to other kinds of constituents. The proportions of constituents migrating into blood were shown in Figure 3. The more detail constituents information was shown in Figure 4.

Moreover, we are surprised to find that the contents of constituents migrating into blood among dosed serum of 30 min, 60 min, and 90 min were interesting. The contents of flavonoids including oroxin A, baicalin, kaempferol 7-O-alpha-L-rhamnopyranoside, luteolin 7,3'-dimethyl ether 5-glucoside, scutellarin, cosmosiin, genkwanol A, and hispidulin, and some other class compounds such as 3-Epilitsenolide D2, asperulosidic acid, helioscopinolide A, 7,8-dihydroxycoumarin, and 7,8-dihydroxy-4-methylcoumarin were rapidly increased to the highest and then sharply decreased in the whole period. However, several flavonoids such as apiin, tiliroside, luteolin-4'-O-glucoside, pratensein-7-O-glucoside, and ent-Robinetinidol, and other compounds such as neochlorogenic acid and 2-hydroxycinnamic acid were hardly present in the front 60 min but promptly increased between 60 min and 90 min. Besides, the two benzopyrans named phomoeuphorbin A and phomoeuphorbin C were

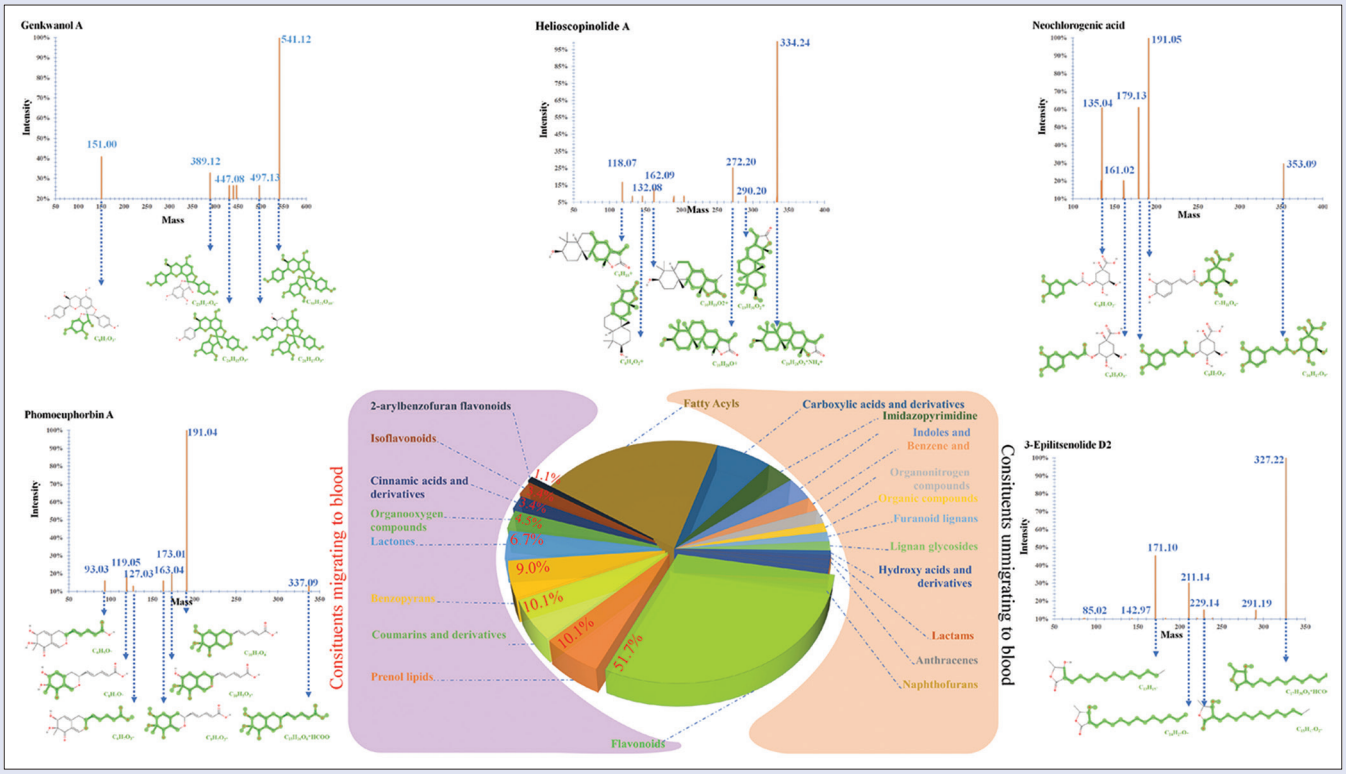

Figure 3: The classification and proportion of constituents and the detail mass spectrometry/mass spectrometry fragments of several constituents migrating into blood of *Shizao* decoction

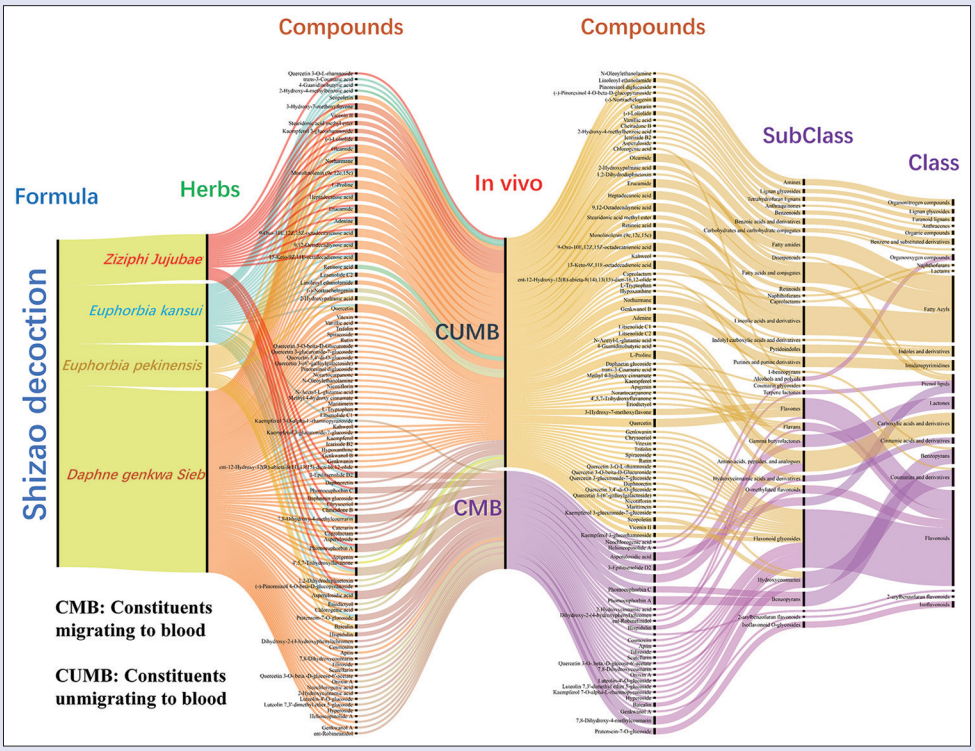

Figure 4: The detail compounds information covering the origin, names, migrating to blood or not, and classification of constituents from *Shizao* decoction in rat serum

first raised then descend and finally raised again. The constituents migrating into blood indicated that the content in different times maybe related with the compound structure and polarity. Take the overall consideration, to detect most constituents, the time point of

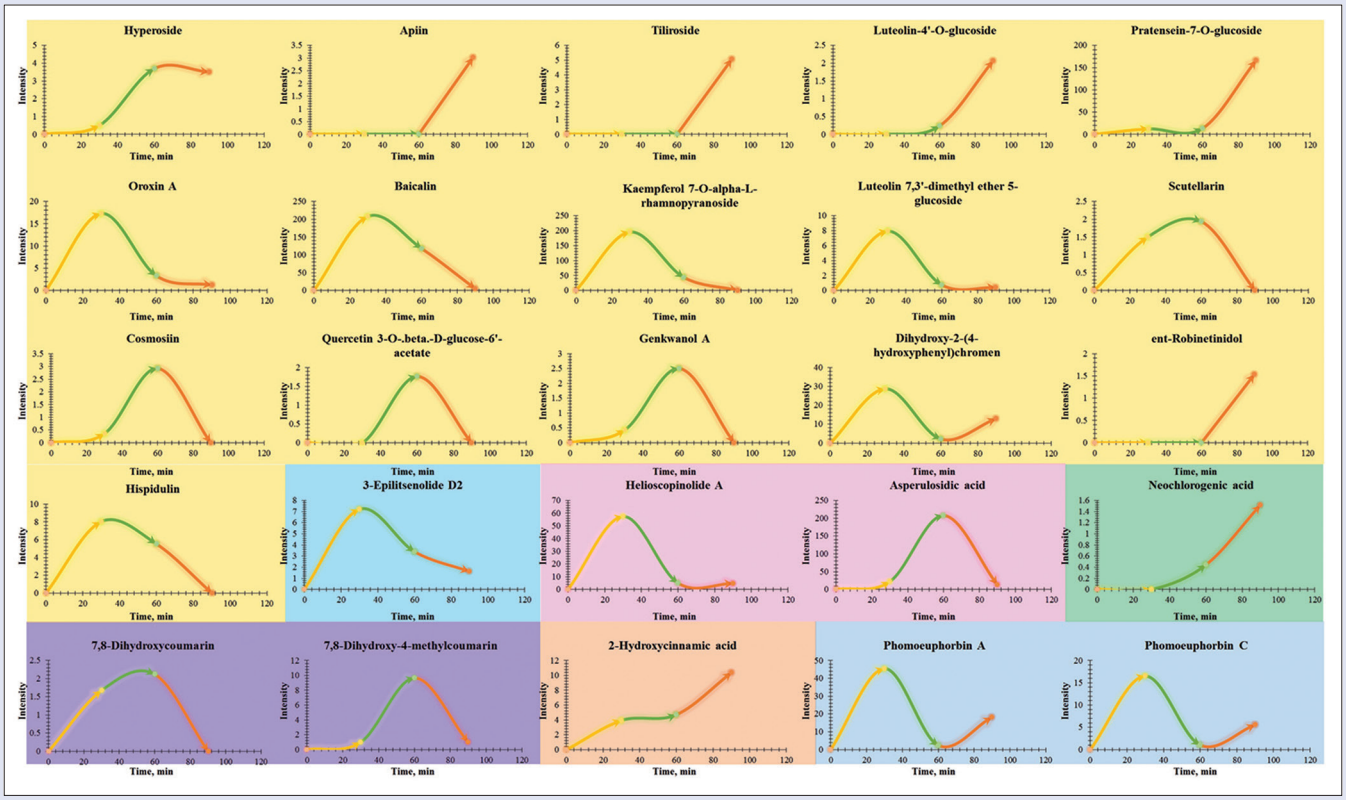

Figure 5: The content trends of constituents migrating into blood after 30, 60, and 90 min. ■: Flavonoids compounds; ■: Lactones compounds; ■: Prenol lipids compounds; ■: Organooxygen compounds; ■: Coumarins and derivatives compounds; ■: Cinnamic acids and derivatives compounds; ■: Benzopyrans

blood collection may be selected at 60 min. The detail results were displayed in Figure 5.

Besides, it is surprised that the majority of constituents migrating into blood showed bright-eyed similar pharmacological actions, especially like anti-cancer. Here, we gave an outline of the modern pharmacological actions of 7,8-dihydroxycoumarin, hyperoside, and scutellarin. 7,8-dihydroxycoumarin, also known as daphnetin, was an active ingredient extracted from *Daphne Korean Nakai,* which usually used for thromboangiitis obliterans and coronary heart diseases. Except for this, modern pharmacological studies showed that 7,8-dihydroxycoumarin expressed distinct activity action in cancer. Kumar *et al.*[22] investigated the antiproliferative and chemotherapeutic actions of 7,8-dihydroxycoumarin against on dimethylbenz (a)anthracene-induced mammary carcinoma SD rats. The results showed that, 20 mg/kg, 40 mg/kg, and 80 mg/kg7,8-dihydroxycoumarin had different levels in alleviating the estrogen synthesis, tumor growth, proliferation markers like Ki-67 and proliferating cell nuclear antigen, cytokines such as interleukin 10 (IL-10), IL-1beta and IL-12, MCP-1chemokine, the expressions of ERalpha, PR, EGFR, IGF1R, p-MAPK1/2, p-JNK1/2, p-Akt, and 17beta-HD1 in mammary carcinoma bearing model rats in a dose-dependent manner. Furthermore, Kumar *et al.*[23] also verified that 7,8-dihydroxycoumarin could against mammary cancer by Nrf-2-Keap1 pathway and NF-kappaB expressions. Besides, Fukuda *et al.*[24] revealed that 7,8-dihydroxycoumarin reduced the numbers of intracellular stress fibers, and filopodia obviously, decreased the expression levels of RhoA and Cdc42dramatically, so that to hold back the invasion and migration of LM8 cells to against the metastatic cancer. Besides, another hot ingredient migrating into blood is hyperoside, a flavonol glycosides often acted out various actions in anticancer,[25-27] anti-inflammation,[28,29] anti-oxidant,[30] etc.[31-33] Zhangand Zhang[34] found that after the intervention of hyperoside, the cell viability and proliferation of titanium particle-induced damage was enhanced, the apoptosis and autophagy of MC3T3E1 cells were dramatically restrained by regulating the TWEAKp38 pathway, indicating that hyperoside may be a potential protective agent for bones. Li *et al.*[35] illustrated that both hyperoside and let-7a-5p had a synergetic effect on suppressing the proliferation of A549 cells, suggesting that the cooperation of hyperoside and microRNA-let7a-5p may provide a novel means for the treatment of lung cancer. Scutellarin, a flavonoid compound firstly extracted from a Chinese herb named *Scutellaria altissima* L., is usually applied in cerebrovascular diseases to reduce the cerebral vascular resistance, improve cerebral blood circulation, increase cerebral blood flow, and reatrain platelet aggregation. Recently, studies have shown that scutellarin owns a variety of activities such as anticancer,[36] antidiabetes,[37] and anti-atherosclerosis.[38,39] Liu *et al.*[40] studied the effect of scutellarin on the proliferation and invasion of hepatocellular carcinoma cells through proliferation, colony-forming, apoptosis and cell migration assays, the result showed that scutellarin could suppress invasiveness of HepG2 and MHCC97-H cells *in vitro* by remodeling their cytoskeleton through inhibiting the process of EMT, so that to down-regulated the JAK2/STAT3 pathway. Furthermore, Cao *et al.*[41] discussed the inhibiting effect of scutellarin on A549 lung adenocarcinoma cells, the data showed that scutellarin restrained the proliferation of A549 cells depend on concentration and time, caused important G0/G1 phase arrest and apoptosis, reduced the level of pan-AKT, phosphorylated (p)-mTOR, mTOR, BCL-XL, STAT3 and p-STAT3, increased the level of 4EBP1, indicating that scutellarin impeded the proliferation and promoted apoptosis of A549 cells through AKT/mTOR/4EBP1 and STAT3 pathways. Sun *et al.*[42] explored that scutellarin could significantly stimulate phosphorylation

of extracellular-regulated kinases 1/2 (ERK1/2), down-regulated the expression of p-AKT to induce the apoptosis and autophagy of non-small cell lung cancer through ERK1/2 and AKT signaling pathways. The study of pharmacodynamic material basis is crucial to elucidate the effect mechanism[43-50] and might provide insight into the characteristics for pharmacological effects.[51-56] In summary, the bioactive constituents migrating into blood such as 7,8-dihydroxycoumarin, hyperoside, and scutellarin expressed multiple activities, especially in anticancer activity. This may work in concert with the modern specific application in cancer of SZD. Hence, 7,8-dihydroxycoumarin, hyperoside, and scutellarin may be the critical constituents even likely to be the pharmacodynamic material basis of SZD in anticancer. However, the suppositional argument needs to be further verified in pharmacological experiment in animals and cells.

CONCLUSION

In this paper, a reliable and sensitive method named UHPLC-ESI-Q-TOF-MS coupled with an automated multivariate analysis approach was applied in the identification and characterization of multiple constituents from SZD. Using this method, 91 compounds of SZD were identified and 25 of them were tentatively characterized. Among the constituents of the SZD sample *in vitro*, most of them were flavonoids. Meantime, among the constituents migrating into blood, more than half of them were flavones as well. These flavones constituents owned multiple activities, especially like anticancer. The result showed the flavones of SZD migrating into blood, especially such as 7,8-dihydroxycoumarin, hyperoside, and scutellarin may play a critical role in pharmacodynamic material basis of SZD in anticancer. Since this paper offered a powerful basis for further pharmacological studies in animals and cells. Anything else, the results also demonstrated that UHPLCESI-Q-TOFMS was a powerful analytical tool in the study of chemical constituents of herbal medicine *in vitro* and *in vivo*. It is worth mentioning that this was the first study of chemical constituents and absorbed bioactive components of SZD. The results not only filled the gaps of the fundamental constituent research of SZD but also offered useful information for further study of pharmacology and mechanism of SZD.

Financial support and sponsorship

The present study was financially supported by Foundation of Heilongjiang Education Department (Grant No. 2018-KYYWF-0080), the projects of Qiqihar Medicinal University (QY2016B-23, QY2016M-13), Key Program of Natural Science Foundation of State (Grant No. 81973745, 81302905), Young Talent Lift Engineering Project of China Association of TCM (QNRC2-B06), Natural Science Foundation of Heilongjiang Province (YQ2019H030), Foundation of Heilongjiang University of Chinese Medicine (2018jc01).

Conflicts of interest

There are no conflicts of interest.

REFERENCES

1. Bo Y, Wang L, Wu X, Zhao L, Yang J, Xiong Z, *et al.* Development and validation of a UHPLC-MS/MS method for the simultaneous determination of five bioactive flavonoids in rat plasma and comparative pharmacokinetic study after oral administration of Xiaochaihu tang and three compatibilities. J Sep Sci 2017;40:1896-905.
2. Liu X, Wang X, Zhu T, Zhu H, Zhu X, Cai H, *et al.* Study on spectrum-effect correlation for screening the effective components in Fangji Huangqi tang basing on ultra-high performance liquid chromatography-mass spectrometry. Phytomedicine 2018;47:81-92.
3. Sun H, Zhang AH, Yang L, Li MX, Fang H, Xie J, *et al.* High-throughput chinmedomics strategy for discovering the quality-markers and potential targets for Yinchenhao decoction. Phytomedicine 2019;54:328-38.
4. Fan Y, Li Y, Wu Y, Li L, Wang Y, Li Y. Identification of the chemical constituents in Simiao wan and rat plasma after oral administration by GC-MS and LC-MS. Evid Based Complement Alternat Med 2017;2017:6781593.
5. Sun H, Chen X, Zhang A, Sakurai T, Jiang J, Wang X. Chromatographic fingerprinting analysis of Zhizhu Wan preparation by high-performance liquid chromatography coupled with photodiode array detector. Pharmacogn Mag 2014;10:470-6.
6. Wang XJ, Zhang AH, Kong L, Yu JB, Gao HL, Liu ZD, *et al.* Rapid discovery of quality-markers from Kaixin San using chinmedomics analysis approach. Phytomedicine 2019;54:371-81.
7. Gao HL, Zhang AH, Yu JB, Sun H, Kong L, Wang XQ, *et al.* High-throughput lipidomics characterize key lipid molecules as potential therapeutic targets of Kaixinsan protects against Alzheimer's disease in APP/PS1 transgenic mice. J Chromatogr B Analyt Technol Biomed Life Sci 2018;1092:286-95.
8. Zhang AH, Yu JB, Sun H, Kong L, Wang XQ, Zhang QY, *et al.* Identifying quality-markers from Shengmai san protects against transgenic mouse model of Alzheimer's disease using Chinmedomics approach. Phytomedicine 2018;45:84-92.
9. Liu Q, Zhang A, Wang L, Yan G, Zhao H, Sun H, *et al.* High-throughput Chinmedomics-based prediction of effective components and targets from herbal medicine AS1350. Sci Rep 2016;6:38437.
10. Nan Y, Zhou X, Liu Q, Zhang A, Guan Y, Lin S, *et al.* Serum metabolomics strategy for understanding pharmacological effects of Shenqi pill acting on kidney yang deficiency syndrome. J Chromatogr B Analyt Technol Biomed Life Sci 2016;1026:217-26.
11. Yang X, Zhang X, Yang SP, Le T, Fan XD, Guo X, *et al.* Simultaneous quantitative analysis of multi-compounds by a single marker in *Radix astragali* by using serum HPLC-MS feature. Pak J Pharm Sci 2016;29:1243-9.
12. Li XN, Zhang A, Wang M, Sun H, Liu Z, Qiu S, *et al.* Screening the active compounds of *Phellodendri amurensis* cortex for treating prostate cancer by high-throughput Chinmedomics. Sci Rep 2017;7:46234.
13. Ju Z, Li J, Han H, Yang L, Wang Z. Analysis of bioactive components and multi-component pharmacokinetics of saponins from the leaves of *Panax notoginseng* in rat plasma after oral administration by LC-MS/MS. J Sep Sci 2018;41:1512-23.
14. Sun H, Liu J, Zhang A, Zhang Y, Meng X, Han Y, *et al.* Characterization of the multiple components of acanthopanax senticosus stem by ultra high performance liquid chromatography with quadrupole time-of-flight tandem mass spectrometry. J Sep Sci 2016;39:496-502.
15. Liu C, Zhang A, Yan GL, Shi H, Sun H, Han Y, *et al.* High-throughput ultra high performance liquid chromatography coupled to quadrupole time-of-flight mass spectrometry method for the rapid analysis and characterization of multiple constituents of *Radix polygalae*. J Sep Sci 2017;40:663-70.
16. Liu Q, Liu J, Fan S, Yang D, Wang H, Wang Y. Rapid discovery and global characterization of multiple components in corn silk using a multivariate data processing approach based on UHPLC coupled with electrospray ionization/quadrupole time-of-flight mass spectrometry. J Sep Sci 2018;41:4022-30.
17. Han Y, Zhang A, Sun H, Zhang Y, Meng X, Yan G, *et al.* High-throughput ultra high performance liquid chromatography combined with mass spectrometry approach for the rapid analysis and characterization of multiple constituents of the fruit of *Acanthopanax senticosus* (Rupr. Et maxim.) harms. J Sep Sci 2017;40:2178-87.
18. Zhang A, Liu Q, Zhao H, Zhou X, Sun H, Nan Y, *et al.* Phenotypic characterization of Nanshi oral liquid alters metabolic signatures during disease prevention. Sci Rep 2016;6:19333.
19. Shu X, Jiang XW, Cheng BC, Ma SC, Chen GY, Yu ZL, *et al.* Ultra-performance liquid chromatography-quadrupole/time-of-flight mass spectrometry analysis of the impact of processing on toxic components of kansui radix. BMC Complement Altern Med 2016;16:73.
20. Qiao Y, Zhao Y, Wu Q, Sun L, Ruan Q, Chen Y, *et al.* Full toxicity assessment of genkwa flos and the underlying mechanism in nematode *Caenorhabditis elegans*. PLoS One 2014;9:e91825.
21. Cao Y, Cheng F, Yao W, Bao B, Zhang K, Zhang L, *et al.* Toxicity of pekinenin C from *Euphorbia pekinensis* radix on rat small intestinal crypt epithelial cell and its apoptotic mechanism. Int J Mol Sci 2016;17. pii: E850.
22. Kumar A, Sunita P, Jha S, Pattanayak SP. 7,8-dihydroxycoumarin exerts antitumor potential on DMBA-induced mammary carcinogenesis by inhibiting ERα, PR, EGFR, and IGF1R: Involvement of MAPK1/2-JNK1/2-akt pathway. J Physiol Biochem 2018;74:223-34.
23. Kumar A, Jha S, Pattanayak SP. Daphnetin ameliorates 7,12-dimethylbenz[a] anthracene-induced mammary carcinogenesis through Nrf-2-Keap1 and NF-κB pathways. Biomed Pharmacother 2016;82:439-48.

24. Fukuda H, Nakamura S, Chisaki Y, Takada T, Toda Y, Murata H, *et al.* Daphnetin inhibits invasion and migration of LM8 murine osteosarcoma cells by decreasing RhoA and cdc42 expression. Biochem Biophys Res Commun 2016;471:63-7.
25. Zhu X, Ji M, Han Y, Guo Y, Zhu W, Gao F, *et al.* PGRMC1-dependent autophagy by hyperoside induces apoptosis and sensitizes ovarian cancer cells to cisplatin treatment. Int J Oncol 2017;50:835-46.
26. Liu Z, Liu G, Liu X, Li S. The effects of hyperoside on apoptosis and the expression of Fas/FasL and survivin in SW579 human thyroid squamous cell carcinoma cell line. Oncol Lett 2017;14:2310-4.
27. Zhou YQ, Zhao YT, Zhao XY, Liang C, Xu YW, Li L, *et al.* Hyperoside suppresses lipopolysaccharide-induced inflammation and apoptosis in human umbilical vein endothelial cells. Curr Med Sci 2018;38:222-8.
28. Yang L, Shen L, Li Y, Li Y, Yu S, Wang S. Hyperoside attenuates dextran sulfate sodium-induced colitis in mice possibly via activation of the Nrf2 signalling pathway. J Inflamm (Lond) 2017;14:25.
29. Liu F, Zhao Y, Lu J, Chen S, Zhang X, Mao W. Hyperoside inhibits proinflammatory cytokines in human lung epithelial cells infected with mycoplasma pneumoniae. Mol Cell Biochem 2019;453:179-86.
30. Chen Y, Ye L, Li W, Li D, Li F. Hyperoside protects human kidney2 cells against oxidative damage induced by oxalic acid. Mol Med Rep 2018;18:486-94.
31. Liu B, Tu Y, He W, Liu Y, Wu W, Fang Q, *et al.* Hyperoside attenuates renal aging and injury induced by D-galactose via inhibiting AMPK-ULK1 signaling-mediated autophagy. Aging (Albany NY) 2018;10:4197-212.
32. Zou L, Chen S, Li L, Wu T. The protective effect of hyperoside on carbon tetrachloride-induced chronic liver fibrosis in mice via upregulation of Nrf2. Exp Toxicol Pathol 2017;69:451-60.
33. An X, Zhang L, Yuan Y, Wang B, Yao Q, Li L, *et al.* Hyperoside pre-treatment prevents glomerular basement membrane damage in diabetic nephropathy by inhibiting podocyte heparanase expression. Sci Rep 2017;7:6413.
34. Zhang Q, Zhang XF. Hyperoside decreases the apoptosis and autophagy rates of osteoblast MC3T3E1 cells by regulating TNFlike weak inducer of apoptosis and the p38mitogen activated protein kinase pathway. Mol Med Rep 2019;19:41-50.
35. Li JP, Liao XH, Xiang Y, Yao A, Song RH, Zhang ZJ, *et al.* Hyperoside and let-7a-5p synergistically inhibits lung cancer cell proliferation via inducing G1/S phase arrest. Gene 2018;679:232-40.
36. Nie J, Yang HM, Sun CY, Liu YL, Zhuo JY, Zhang ZB, *et al.* Scutellarin enhances antitumor effects and attenuates the toxicity of bleomycin in H22 ascites tumor-bearing mice. Front Pharmacol 2018;9:615.
37. Liu Y, Wang J, Zhang X, Wang L, Hao T, Cheng Y, *et al.* Scutellarin exerts hypoglycemic and renal protective effects in db/db mice via the nrf2/HO-1 signaling pathway. Oxid Med Cell Longev 2019;2019:1354345.
38. Fu Y, Sun S, Sun H, Peng J, Ma X, Bao L, *et al.* Scutellarin exerts protective effects against atherosclerosis in rats by regulating the hippo-FOXO3A and PI3K/AKT signaling pathways. J Cell Physiol 2019;234:18131-45.
39. Ding D, Cai X, Zheng H, Guo SW, Liu X. Scutellarin suppresses platelet aggregation and stalls lesional progression in mouse with induced endometriosis. Reprod Sci 2018. doi. org/10.1177/1933719118817661.
40. Liu K, Tian T, Zheng Y, Zhou L, Dai C, Wang M, *et al.* Scutellarin inhibits proliferation and invasion of hepatocellular carcinoma cells via down-regulation of JAK2/STAT3 pathway. J Cell Mol Med 2019;23:3040-4.
41. Cao P, Liu B, Du F, Li D, Wang Y, Yan X, *et al.* Scutellarin suppresses proliferation and promotes apoptosis in A549 lung adenocarcinoma cells via AKT/mTOR/4EBP1 and STAT3 pathways. Thorac Cancer 2019;10:492-500.
42. Sun C, Li C, Li X, Zhu Y, Su Z, Wang X, *et al.* Scutellarin induces apoptosis and autophagy in NSCLC cells through ERK1/2 and AKT signaling pathways *in vitro* and *in vivo*. J Cancer 2018;9:3247-56.
43. Huang CG, Shang YJ, Zhang J, Zhang JR, Li WJ, Jiao BH. Hypouricemic effects of phenylpropanoid glycosides acteoside of *Scrophularia ningpoensis* on serum uric acid levels in potassium oxonate-pretreated mice. Am J Chin Med 2008;36:149-57.
44. Wang XJ, Ren JL, Zhang AH, Sun H, Yan GL, Han Y, *et al.* Novel applications of mass spectrometry-based metabolomics in herbal medicines and its active ingredients: Current evidence. Mass Spectrom Rev 2019;38:380-402.
45. Zhang HL, Zhang A, Miao JH, Sun H, Yan GL, Wu FF, *et al.* Targeting regulation of tryptophan metabolism for colorectal cancer therapy: A systematic review. RSC Adv 2019;9:338-72.
46. Zhang A, Yan G, Han Y, Wang X. Metabolomics approaches and applications in prostate cancer research. Appl Biochem Biotechnol 2014;174:6-12.
47. Sun H, Zhang AH, Liu SB, Qiu S, Li XN, Zhang TL, *et al.* Cell metabolomics identify regulatory pathways and targets of magnoline against prostate cancer. J Chromatogr B Analyt Technol Biomed Life Sci 2018;1102-1103:143-51.
48. Li X, Zhang A, Sun H, Liu Z, Zhang T, Qiu S, *et al.* Metabolic characterization and pathway analysis of berberine protects against prostate cancer. Oncotarget 2017;8:65022-41.
49. Li YF, Qiu S, Gao LJ, Zhang AH. Metabolomic estimation of the diagnosis of hepatocellular carcinoma based on ultrahigh performance liquid chromatography coupled with time-of-flight mass spectrometry. RSC Adv 2018;17:9375-82.
50. Du HW, Zhao XL, Zhang AH. Identifying potential therapeutic targets of a natural product Jujuboside B for insomnia through network pharmacology. Plant Sci Today 2014;1:69-79.
51. Fang H, Zhang AH, Sun H, Yu JB, Wang L, Wang XJ. High-throughput metabolomics screen coupled with multivariate statistical analysis identifies therapeutic targets in alcoholic liver disease rats using liquid chromatography-mass spectrometry. J Chromatogr B Analyt Technol Biomed Life Sci 2019;1109:112-20.
52. Zhang YL, Liu P, Li YF, Zhang AH. Exploration of metabolite signatures using high-throughput mass spectrometry coupled with multivariate data analysis. RSC Adv 2017;7:6780-7.
53. Sun H, Zhang HL, Zhang A, Zhou XH, Wang X, Han Y, *et al.* Network pharmacology combined with functional metabolomics discover bile acid metabolism as a promising target for mirabilite against colorectal cancer. RSC Adv 2018;8:30061-70.
54. Sun H, Zhang AH, Song Q, Fang H, Liu XY, Su J, *et al.* Functional metabolomics discover pentose and glucuronate interconversion pathways as promising targets for Yang Huang syndrome treatment with Yinchenhao Tang. RSC Adv 2018;8:36831-9.
55. Zhang AH, Sun H, Yan GL, Han Y, Zhao QQ, Wang XJ. Chinmedomics: A powerful approach integrating metabolomics with serum pharmacochemistry to evaluate the efficacy of traditional Chinese medicine. Engineering 2019;5:60-8.
56. Wang XJ, Li J, Zhang AH. Urine metabolic phenotypes analysis of extrahepatic cholangiocarcinoma disease using ultra-high performance liquid chromatography-mass spectrometry. RSC Adv 2016;6:63049-57.